Virus structure analysis with synchrotron radiation: methods and results

John E. Johnson

Department of Molecular Biology, The Scripps Research Institute, 10550 N. Torrey Pines Rd. La Jolla, CA 92037, USA. E-mail: jackj@scripps.edu

Structural studies of viruses that are investigated as part of a program to understand molecular machines are described. Crystallography, solution x-ray scattering, electron microscopy and molecular virology were employed to investigate structure, assembly and maturation of RNA and dsDNA viruses. 240 copies of the RNA viral subunits (each with 650 amino acids) spontaneously assemble at pH 7 in a baculovirus expression system to form *T*=4 icosahedral particles, 450Å in diameter. At pH 5 the particles condense to 410Å and the subunits auto-catalytically cleave at residue 570. 420 copies of the dsDNA viral subunits (281 amino acids each) assemble in an *E. coli* expression system to form T=7 icosahedral particles, 450Å in diameter. At pH 4 the particles expand to 650Å diameter with the auto-catalytic formation of cross links between a lysine side chain and an asparagine side chain creating a concatenated set of 60 hexamer and 12 pentamer rings rendering the particle impervious to denaturation without protease treatment. We have determined moderate to high resolution structures of the procapsids and capsids of these virus particles as well as cryoEM reconstructions of intermediate structures in order to define the driving force and the trajectories of these large-scale transitions.

Keywords: HK97; tetraviruses; virus structure; virus dynamics; virus crystallography.

1. Introduction

Viruses are two-edged swords as they relate to humans. Many are dangerous pathogens that cause extraordinary human suffering, mortality and economic loss (e.g HIV and SARS). Viruses benign to humans, however, also provide the means for understanding numerous biological processes that, by analogy, lead to an understanding of cellular functions crucial for the development of therapies for disease. More recently some benign viruses were recognized as viable reagents for applications in nano technology, chemistry and biology (Douglas & Young, 1998, Wang, et al., 2002a, Wang, et al., 2002b, Wang, et al., 2002c). We investigate virus capsids in this arena with synchrotron radiation and crystallography as well as by electron microscopy and molecular virology. Through these studies we discovered novel and in some cases unique properties of macromolecular organizations and dynamics. Here we discuss results obtained with a capsid that normally packages the genome of a single strand RNA virus and one that normally packages a double strand DNA genome. Employing methods of genetic engineering and protein expression we were able to produce these capsids without packaged genomic nucleic acid and at levels much higher than they are produced in an infection. These virus shells are not infectious and are dynamic nano particles that are used as bio materials. The capsids range in size from 410Å for the RNA virus to 650Å for the dsDNA virus and they form well-ordered crystals with proportionally large unit cells. The weak diffraction from these crystals and the closely spaced diffraction maxima require synchrotron radiation for the collection of high quality data. Dynamic features of these transitions were investigated with solution x-ray scattering.

2. RNA virus capsid polymorphism

Nudaurelia ω Capensis virus (NωV) has a coat protein gene encoding 644 amino acids. The capsid contains 240 copies of the subunit arranged with a T=4 quasi-symmetric surface lattice. Authentic virus was characterized by crystallography in a compact, 410Å diameter form, but expression of the capsid protein gene in a baculovirus system generates a particle that can exist at pH 7.0 with a 450Å diameter and a compact form, at pH 5.0 (Figure 1), that is indistinguishable from authentic particles (Canady, et al., 2000). Synchrotron solution x-ray scattering was used to determine a titration curve (Figure 2) for the transition that is sharply defined between pH values of 6.5 and 5.5 (Canady, et al., 2001). The large particle was only observed in an artificial expression/assembly system and it must be determined if it is an interesting and useful artifact or of consequence in the virus life cycle. NωV and other tetraviruses are the only known examples of non-enveloped T=4 ssRNA viruses that undergo such a transition. Since these particles require subunits to exist in four structurally unique environments within the icosahedral asymmetric unit, it may be necessary for them to assemble in stages that include a procapsid form. If this hypothesis is correct, it may be expected that the pH of wild-type virus could be raised, thus generating the expanded putative procapsid. This does not occur because the low pH form of the virus undergoes an auto proteolysis in which cleavage (Figure 1) occurs at residue 570 (Agrawal & Johnson, 1995). The cleaved polypeptide (residues 571-644) remains associated with the particle (Munshi, et al., 1996), but the cleavage "locks" the capsid state and it can not be reversed (Canady, et al., 2001). The auto proteolysis occurs in particles produced in the expression/assembly system when they are lowered to pH 5 and in authentic virus. Recently it was shown that the transition is reversible if the cleavage is inhibited by mutating ASN570 to THR, although there is an obvious hysteresis when the forward and reverse conversions are compared (Taylor, et al., 2002). It is now possible to produce substantial amounts of these particles in the expression system. The reversible mutation is one of the most efficient genes expressed with 50-milligram preparations of particles now possible. Attaching appropriate fluorescent probes to these particles may allow them to be used as sensors. Mutant particles may also be used as proton driven reversible nano engines that may be coupled to other devices.

3. DNA virus capsid polymorphism

HK97 is a dsDNA bacterial virus similar to phage λ. It undergoes a remarkable morphogenesis in its assembly and maturation and this process can be recapitulated in vitro. 420 copies of the dsDNA viral subunits (281 amino acids each) assemble in an *E. coli* expression system to form T=7 icosahedral particles, 450Å in diameter (Hendrix & Duda, 1998). The most dramatic event is the expansion from prohead II (~450Å in size) to head (~650Å) that occurs when the pH of prohead II is lowered from 7 to 4. Both particles have identical protein composition (Lata, et al., 2000). We determined the atomic resolution structure of the mature particle and discovered the mechanism used to concatenate the subunits of the particle into a chain-mail fabric similar to that seen in armor of medieval knights (Wikoff, et al., 2000). This required an exceptionally difficult structure determination from crystals with a very large unit cell (Wikoff, et al., 1998, Wikoff, et al., 1999). Figure 3 shows a diffraction pattern from the HK97 head crystals and Table I shows the data collection statistics. Figure 4 shows the resulting structure and the unique topological organization of the viral subunits that are covalently linked together by a bond between lysine and asparagine side chains that form by an auto catalytic reaction when the capsid expands. We have also examined the

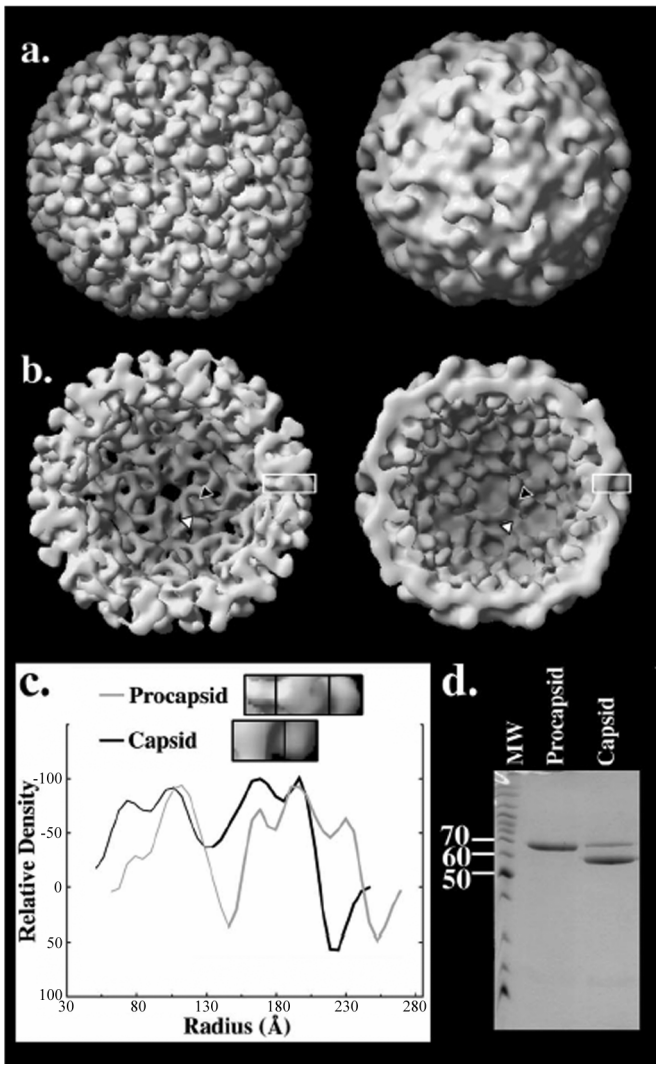

Figure 1

Three-dimensional, surface-shaded views of (a) the full particle and (b) sectioned views of the procapsid (left) and capsid(right) of NwV VLPs viewed down a 2-fold symmetry axis, with 3-fold (black triangle) and quasi 3-fold (white triangle) axes marked in (b). The procapsid is larger, rounded, and porous, while the mature capsid has a smaller, angular, solid shell. (c) The radial density plots reveal that the capsid protein shell (black line) spanned 62Å with two domains, whereas the procapsid (gray line) had a thickness of 83Å and comprised three domains. A cross-section of each map is shown above the plot, the domains delineated and placed in register with the radii to which they correspond. (d) An SDS-PAGE gel showing that the procapsid sample contains the 70 kD uncleaved coat protein, while the capsid contains mostly 62 kDa and 8 kDa (not visible) coat protein fragments which result from autoproteolysis upon lowering of the pH to 5.0 (Canady, et al., 2000).

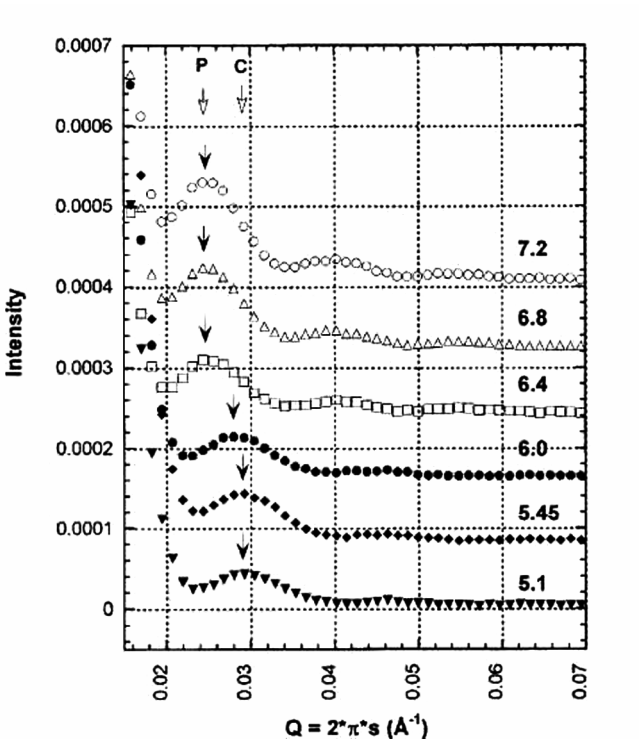

Figure 2

Linear plots of NωV Virus-Like-Particles (VLP) SAX curves recorded at fixed pH values. Scattering curves were measured on a procapsid VLP sample that was dialyzed against progressively lower pH values. The VLP sample began at pH 7.6 and was dialyzed at the pH values indicated on the curves. The positions of the first scattering peaks of the procapsid (P) and capsid (C) are indicated at the top with white-tipped arrows, and the position of the first peak for each sample curve is indicated above it with a black-tipped arrow. The position of the first peak for the pH 7.2, 6.8, and 6.4 samples (open symbols) indicates that they are in the procapsid state, while the pH 5.45 and 5.1 samples (filled symbols) are in the capsid state. The first peak for the sample at pH 6.0 (gray symbol) indicates a particle radius of 205Å , but the curve could be closely approximated by a linear combination of the pH 6.4 and pH 5.45 scattering curves, indicating that it probably results from a mixed population of procapsid and capsid. Scattering data (except the pH 5.1 curve) were offset on the vertical axis for ease of viewing. Solution scattering data were collected at the Stanford Synchrotron Radiation Laboratory as described (Canady, et al., 2001).

expansion of the particle with time-resolved solution x-ray scattering and electron cryo microscopy (Lata, et al., 2000). Solution x-ray scattering studies of the transition at pH 4.0, that were recorded at one-minute intervals, indicated that, while the transition was rapid, it was stochastic. The expansion had a half-life of roughly 10 minutes, but only two states were detected at any given time, as the curves displayed isosbestic points and were readily interpreted as linear combinations of scattering from only two states. This indicated that the transitions between states occurred in less than the intervals of solution scattering data collection, but that the individual expansion events occurred randomly with a half-life of 10 minutes. Studies with electron cryo microscopy comparing the prohead II state and the final head II state show that rigid-body rotations (~40 degrees) of the protein subunits cause switching to an entirely different set of protein-protein interactions; in addition, two polypeptide regions undergo significant refolding. These changes stabilize the capsid by increasing the surface area buried at interfaces and bringing the cross-link–forming residues, initially 40 angstroms apart, close together. The inner surface of Prohead-II is negatively charged, suggesting that DNA packaging triggers the transition electrostatically (Conway, et al., 2001).

4. Conclusions

Virus maturation provides readily accessible systems for the study of large-scale protein transitions that characterize many processes in biology. The two processes described here are both triggered by

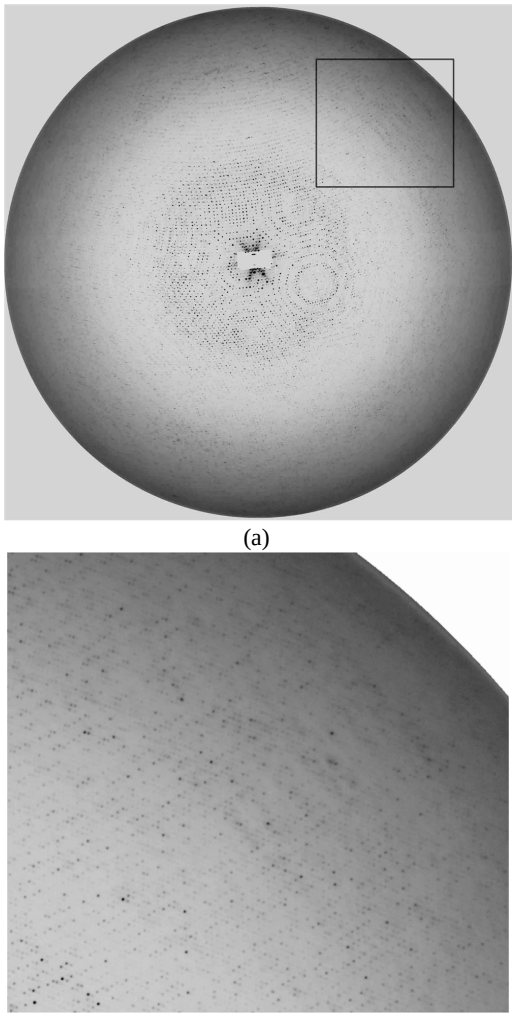

(a)

(b)

Figure 3

Single crystal diffraction from HK97 crystals. (a) An HK97 Head II diffraction pattern collected on the MAR345 detector at the Advanced Photon Source, beamline 14-BM-C at a wavelength of 1.04 A. The oscillation angle was 0.15° with an exposure time of 45 s. The crystal-to-detector distance was 555 mm. The boxed area in (a) is magnified in (b) showing a detail of the diffraction image. The image was processed to a resolution of 3.45 Å. A total of 1935 whole reflections and 49,001 partial reflections were measured on the image.

Table 1

I HK97 Head II Structure Determination

Space Group: $P2_1$
Lattice Constants: a = 581Å, b = 628Å, c = 789Å, β = 89.9°
Data set recorded on Bio Cars beamline 14BM-C APS
Temperature of data collection: 4°C
Number of crystals: ~200
Number of images recorded (Mar 345): 760 (osc ang 0.25°)
Number of reflections measured: 21,863,976
Number of unique reflections: 4,800,765
Completeness of data: 90Å-3.4Å 63%
Minimum partial accepted: 0.5
Rmerge: 16%
Structure determination: molecular replacement and phase extension starting with the cryoEM reconstruction of head II
MR Rfactor: 32% (real space averaging and phase extension from 20Å to 3.4Å; 60-fold redundancy)
MR CC: 0.85

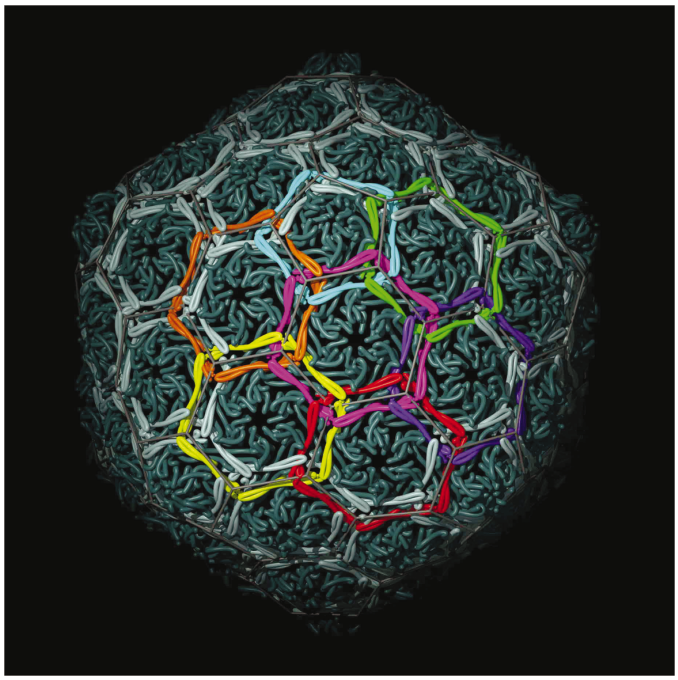

Figure 4

The mature, T=7*l* icosahedral head II form of the bacteriophage HK97 determined at 3.4Å. Head II is the only reported example of protein concatamers stabilizing a quaternary structure. There are 420 covalent, inter subunit cross-links formed between lysine 169 and asparagine 356. These cross links form by an auto catalytic mechanism that occurs during particle maturation. Because the rings occur on both sides of 2-fold, particle symmetry axes, they must "chain-link" to preserve the symmetry (Wikoff, et al., 2000).

increases in proton concentration but are different in character. The NωV transition is reversible when the post maturation cleavage is stopped by the site directed mutation N570T. The current working hypothesis describes a helix (pH above 7) to coil (pH 5) transition of residues 571-644 as the driving force for the transition. When these residues are uncoupled from the remainder of the protein by the autocatalytic cleavage they still change secondary structure as the pH changes, but since they are disconnected from the body of the protein (cargo) in the normal cleavage, it is not reversible. Keeping these residues attached by mutagenesis of the cleavage site makes the reaction reversible (Taylor, et al., 2002).

In contrast, the maturation of HK97 is not reversible when the transition proceeds beyond the local energy minimum trapped by the remodeling of the original assembly product prohead I. Prohead I assembles from hexamers and pentamers of the capsid protein and about 50 copies of a protease encoded by the viral genome that are inside the protein shell. The protease becomes active on assembly and cleaves residues 1-102 from all the capsid proteins. The protease then auto-digests and all the resulting polypeptides diffuse through pores in the particle, making the particle empty (Hendrix & Duda, 1998). Although totally remodeled on the interior, this particle maintains the same external morphology, but is remarkably different from the originally assembled particle. It has changed from a global energy minimum to a local minimum. It is stable in this state indefinitely if not perturbed. Lowering the pH below 4.5, adding any of a variety of mild denaturants or introducing DNA,

however, lifts the particle from the local minimum and allows it to mature to the final icosahedral form that is at a global energy minimum (Duda, et al., 1995).

Analysis of these systems continues with high resolution and stopped-flow time resolved spectroscopy and solution x-ray scattering to map the tertiary and quaternary features of the transitions, allowing the detailed trajectories to be defined. If this is achieved, similar approaches can be applied to less accessible transitory interactions in biology.

The author thanks his collaborators on the NωV studies described, Mary Canady, Derek Taylor, Anette Schneemann, Mark Yeager and Hiro Tsuruta, and his collaborators on the HK97 studies described, William Wikoff, Lars Liljas, Robert Duda, and Roger Hendrix. The BioCARS staff at APS are gratefully acknowledged for their outstanding support in the HK97 data collection. The work was supported by NIH grants AI40101 and GM54076 to JEJ. Use of the Advanced Photon Source was supported by the US Department of Energy, Basic Energy Sciences, Office of Science, under contract No. W 31-109-Eng-38. Use of the BioCARS Sector 14 was supported by the National Institutes of Health, National Center for Research Resources, under grant No. RR-07707. SSRL is operated by the US Department of Energy, Office of Basic Energy Sciences. The SSRL Structural Molecular Biology Program is supported by the US National Institutes of Health, NCRR, and by the DOE OBER.

References

Agrawal, D. &Johnson, J. (1995), *Virology* **207,** 89-97.

Canady, M., Tsuruta, H. &Johnson, J. (2001), *J. Mol. Biol.* **311,** 803-814.

Canady, M. A., Tihova, M., Hanzlik, T. N., Johnson, J. E. &Yeager, M. (2000), *J Mol Biol* **299,** 573-584.

Conway, J., Wikoff, W., Cheng, N., Duda, R., Hendrix, R., Johnson, J. &Steven, A. (2001), *Science* **292,** 744-748.

Douglas, T. &Young, M. (1998), *Nature* **393,** 152-155.

Duda, R. L., Hempel, J., Michel, H., Shabanowitz, J., Hunt, D. &Hendrix, R. W. (1995), *J Mol Biol* **247,** 618-35.

Hendrix, R. W. &Duda, R. L. (1998), *Adv Virus Res* **50,** 235-88.

Lata, R., Conway, J. F., Cheng, N., Duda, R. L., Hendrix, R. W., Wikoff, W. R., Johnson, J. E., Tsuruta, H. &Steven, A. C. (2000), *Cell* **100,** 253-63.

Munshi, S., Liljas, L., Cavarelli, W., Bomu, W., McKinney, B., Reddy, V. &Johnson, J. (1996), *J. Mol. Biol.* **261,** 1-10.

Taylor, D. J., Krishna, N. K., Canady, M. A., Schneemann, A. &Johnson, J. E. (2002), *J Virol* **76,** 9972-80.

Wang, Q., Kaltgrad, E., Lin, T., Johnson, J. &Finn, M. (2002a), *Chemistry and Biology* **9,** 805-811.

Wang, Q., Lin, T., Johnson, J. &Finn, M. (2002b), *Angew. Chem. Int. Ed.* **41,** 459-462.

Wang, Q., Lin, T., Johnson, J. &Finn, M. (2002c), *Chemistry and Biology* **9,** 813-819.

Wikoff, W., Duda, R., Hendrix, R. &Johnson, J. (1998), *Viorolgy* **243,** 113-118.

Wikoff, W., Duda, R., Hendrix, R. &Johnson, J. (1999), *Acta Cryst* **D55,** 763-771.

Wikoff, W., Liljas, L., Duda, R., Tsuruta, H., Hendrix, R. &Johnson, J. (2000), *Science* **289,** 2129-2133.